DOI: https://dx.doi.org/10.4314/gjgs.v21i1.7

GLOBAL JOURNAL OF GEOLOGICAL SCIENCES VOL. 21, 2023: 91-115
COPYRIGHT© BACHUDO SCIENCE CO. LTD PRINTED IN NIGERIA ISSN 1596-6798
www.globaljournalseries.com.ng, Email: globaljournalseries@gmail.com

TRACE ELEMENT GEOCHEMICAL IMPRINTS AND MULTI-PATH HEALTH RISK ASSESSMENT OF POTENTIALLY TOXIC ELEMENTS IN SOILS FROM THE POLYMETALLIC AREA OF TASHAN-JATAU, NORTHWESTERN NIGERIA

B. O. OMANG, H. EFFIOM, M. E. OMEKA, P. E. OKO, E. A. ASINYA, L. T. OJIKUTU AND G. T. KAVE

(Received 9 November 2022; Revision Accepted 11 January 2023)

ABSTRACT

The occurrence of Potentially toxic elements (PTEs) in the soil phase may portend environmental, ecological and health-related risks. Hence, this study has combined high-precision geochemical analyses (X-ray fluorescence (XRF) and inductively Coupled Plasma Mass Spectrometry (ICP-MS)), quantitative soil pollution indices and health risk assessment modelling for a holistic and precise assessment of the intrinsic vulnerability of the soil system to contamination. Geochemical analysis showed that the soils are highly enriched with PTEs such as V (mean = 449.5 mg/L), Cr (mean = 529.9 mg/L), Cu (mean = 374.4 mg/L), Sr (mean = 1365.3 mg/L), Zr (mean = 2703 mg/L), Zn (mean = 282.5 mg/L), and Pb (mean = 127.3 mg/L). Quantitative soil pollution assessment (contamination factor and enrichment factor) revealed that besides mining, the distribution and association between trace elements and oxides were from surface environmental conditions (including mobility potential, leaching metal-complexation, weathering and oxidation of parent material). Health risk assessment based on hazard quotient and hazard index revealed that the inhabitants are generally more exposed to risks from toxic elements ingestion than dermal contact and inhalation; the children are vulnerable to risks than adults. The cancer risks from ingestion and dermal contact of As and Cr for both children and adults are relatively higher (> 1.0E−04) than the acceptable range; although the children population seems to be more susceptible to cancer risks due to lower body weight.

KEYWORDS: Potentially toxic elements (PTEs); Contamination factor; Health risk assessment; Mine wastes

INTRODUCTION

The contamination of valued environmental components (VECs) (e.g., soil, air, and water) has become a prevalent environmental and ecological concern especially in the recent Anthropocene and post-industrial age. Exposure of the valued environmental components to pollution have been attributed to a myriad of sources such as mining, agriculture, industrialization etc.

Irrespective of the pollution source, the soil component appears to be the primary repository of contaminant chemical element; as it forms the major part of the nexus that exists between the soil-water interface (Omeka and Egbueri 2022). It therefore suffices to say that the soil component only acts as temporary repository of potentially toxic elements (PTEs); after which other environmental factors such as rainfall, weathering, hydrolysis may enhance their movement into the surface and groundwater system

---

B. O. Omang, Department of Geology, University of Calabar, P.M.B. 1115, Calabar, Cross River State, Nigeria
H. Effiom, Department of Geology, University of Calabar, P.M.B. 1115, Calabar, Cross River State, Nigeria
M. E. Omeka, Department of Geology, University of Calabar, P.M.B. 1115, Calabar, Cross
P. E. Oko, Department of Environmental Resources Management, University of Calabar, Cross River State, Nigeria
E. A. Asinya, Department of Geology, University of Calabar, P.M.B. 1115, Calabar, Cross River State, Nigeria
L. T. Ojikutu, Department of Geology, University of Calabar, P.M.B. 1115, Calabar, Cross River State, Nigeria
G. T. Kave, Department of Geology, University of Calabar, P.M.B. 1115, Calabar, Cross River State, Nigeria

through run-off, infiltration or percolation (Krishna and Mohan, 2016; Xiaodong 2019; Omeka et al. 2022a, b). Moreover, these PTEs may contaminate agricultural lands, and through complex geochemical processes can be taken up by crop plant tissues through the root system (Souri et al., 2018). It is agreed that among these PTEs, some elements (such as Zn, Al, Fe, Mn, and Cu) may serve as essential and major components for plant growth and functionality (Nganje et al., 2021; Omeka and Igwe, 2021). However, their toxicity potential to plants and humans, therefore, becomes significant when they occur in high concentrations (Adepoju-Bello et al. 2009). The high environmental pollution potential of PTEs has been attributed to their high persistence and indestructibility (Pourret et al. 2021).

A myriad of health challenges has been reported from the long-term accumulation, inhalation and ingestion of toxic elements by humans. Cardiovascular issues, breast, lung cancer, and neurological disorders have been reported from the long-term ingestion of Cu, Cd and Pb (Khan et al., 2013; US-EPA, 2017). According to the 2018 toxicological profiling of toxic elements by the Agency of Toxic Substances Disease and Registry (ATSDR, 2018), Cd, Pb, As, and Cr have been grouped under the top ten carcinogenic elements. Life-threatening illnesses such as anaemia, kidney diseases and psychosis have been reported from the short-term and long-term exposure to Cd, Pb and As respectively. Disruption in human foetal development and memory loss in children have also been attributed to Cd and Pb ingestion by humans (Tchounwou et al., 2012; US-EPA, 2017; Okamkpa et al. 2022). Exposure to toxic elements from soils may follow multi-paths such as inhalation of dust particles ingestion, and dermal contact during mining operations and land cultivation. Moreover, toxic elements can be ingested indirectly via the feeding chain (through the consumption of contaminated fruits and crops) (Lu et al. 2014). It is therefore important to carry out a proper geochemical characterization, distribution and assessment of the soil, which serves as the primary target of contamination exposure, for adequate environmental protection and remediation of contaminated sites.

Given the rather complex and dynamic geochemical processes involved in soil contamination, using only conventional methods and legislative guidelines in soil contamination assessment is usually inadequate for a holistic soil contamination assessment, monitoring and environmental protection. Previous studies on soil contamination assessment have relied on the use of conventional methods such as total metal concentration of soil and soil physicochemical parameters such as soil pH, organic matter content, loss on ignition (LOI) etc. (Sparks, 2005; Nganje et al., 2010; Pam, 2013; Obiora et al., 2016). In addition, several legislative guideline values have been set up both locally and internationally to serve as checks on soil contamination status and for regular soil monitoring (CCME, 1999; DPR, 2002; EA 2009; US-EPA, 2005). Similar to the conventional method of soil contamination assessment, these guidelines are dependent on the soil's total metal content. There is a general consensus by some researchers that the use of only the total metal content in soil contamination assessment can lead to either over-exaggeration or underestimation of the environmental and human exposure to trace and potentially toxic element pollution. As such, excessive financial and expat efforts will need to be put into monitoring and remediation of contaminated sites (Li et al., 2009; Jamshidi-Zanjani et al., 2015; Jahromi et al., 2020). Therefore, to carry out a holistic and precise assessment of the intrinsic vulnerability of the soil system to contamination will require an integrated unconventional and multi-criteria study approach. Hence, in this study, we have combined a high precision geochemical analysis (x-ray fluorescence (XRF) and inductively Coupled Plasma Mass Spectrometry (ICP-MS), multiple numerical environmental pollution indices (contamination factor (CF) pollution load index and enrichment factor (EF)) and a composite health risk assessment modelling for multiple exposure pathways (such as inhalation, ingestion and dermal contact) for two human population sizes (adult and children). Most studies on soil total soil metal content extraction are based used digestion and extraction of the metal fraction using nitric acid (HNO_3), aqua regia, and ethylene diamine tetra acetic acid (EDTA) as reagents, extractants and chelating agents respectively (Kim et al. 2009; Jamshidi-Zanjani et al. 2015; Omeka et al. 2022a). The content of the heavy metals has also been determined from the extracts using the atomic absorption spectrophotometer (AAS) fused with the air acetylene flame (Ho and Tai 1988; Omeka and Igwe 2021; Omeka et al. 2022a). The advantage of the XRF and ICP-MS over the AAS is that the non-destructive chemical analysis of rocks, soils, minerals, sediments and fluids can be routinely carried out. This is because the instrument works on wavelength-dispersive spectroscopic principles that are similar to an electron microprobe (EPMA). Moreover, the determination of total or near a total concentration of the trace elements and major oxides in soils and sediments can be determined using XRF, unlike the AAS which can only determine the metal fractions from digested soil extracts. On the other hand, ICP-MS can be useful in determining low concentration (in parts per billion) and ultra-low concentration of elements (in parts per trillion). In addition, unlike the AAS, the ICP-MS has an extremely low detection limit, a large linear range and an ability to detect the isotopic composition of elements (Funtua, 2001). Hence transition metals, such as Vanadium (V), Yttrium (Y), Hafnium (Hf), Zirconium (Zr), Niobium (Nb), Chromium (Cr), Strontium (Sr) etc. may otherwise be undetected using the AAS, can be efficiently identified using the ICP-MS analytical method. Since humans appear to be the immediate recipients of toxic element exposure, an assessment of carcinogenic and non-carcinogenic health risks quotients becomes integral to adequate human health protection. Hence, multiple health risk assessment indices such as average daily dose dermal contact (ADD_{der}), average daily dose inhalation (ADD_{inh}), average daily dose ingestion (ADD_{ing}), hazard quotient (HQ), hazard index (HI) and lifetime cancer risk (LCR) have been used to assess the extent and potential of exposure of humans to metal toxicity. Given the rather complex and dynamic processes involved in metal pollution in, parametric multivariate statistical models (such as principal component analysis) have also been integrated to identify the prevalent pollution source as well as the intrinsic associations between the metals and their associated oxides in the soil.

The Tashan Jatau mine province where the study was carried out occurs within the central portion of the Nigerian basement complex, saddled with intensive artisanal mining activities for Gold. The ore of interest (Gold) is recovered from stream sediments, open pits and weathered rocks by employing primitive and semi-mechanized exploitation methods. The mining methods used do not conform to the set environmental regulations; the mining method involves an open cast method where a large soil material or overburden is excavated to extract the ore of interest (Fig. 1). The excavated overburden may contain waste materials enriched with sulphide minerals composed of PTEs (Cd, Pb, As, Cr, Ni, Hg etc.) in trace quantity. These elements have the propensity to sorb onto soil particles forming metal ligands and complexes; and due to their persistence may bioaccumulate in the soil phase and maintain a long residence time within the soil media (El-Amari et al., 2014; Omeka and Igwe 2021; Omeka et al. 2022a). Apart from artisanal mining, animal husbandry (e.g. nomadic cattle rearing,) and subsistent agricultural activities (e.g. cultivation of perennial crops like yam, rice, millet, guinea corn, cowpea and groundnuts) make part of the occupation of the inhabitants. The mine waste materials are being poorly disposed of forming an extensive pyramid of overburden. The topography of the area is highly undulated; comprising of high hills and occasional low lands. Most of the arable farmlands are found in low-land areas. During intensive rainfall activities, most of the mine spoils are washed off downslope, into farmlands, rivers and other water bodies, thereby constituting a contamination source. Additionally, the local artisanal miners can be exposed to risk from toxic elements during mining operations through inhalation of dust particles, dermal contact and ingestion. Consumers of fruits and crop plants from farmlands adjacent to the mine sites may be exposed to the risk of metal contamination directly through the feeding chain (through the consumption of vegetables, fruits and crops). The animals such as cattle can also be exposed to toxic metal ingestion through their feeding habits; thereby constituting a plant-animal-human pathway of toxic element contamination. No research has been carried out on the geochemical assessment of trace elements in this region. Moreover, there is no literature addressing the extent of soil pollution by toxic elements and the associated human health risks from their exposure thereof. Therefore, this research aims to carry out a preliminary investigation on the distribution, the extent of pollution and the likely associations between chemical elements and oxides as well as the likely sources of pollution within the Tashan Jatau gold mine province. The potential health risk implications from toxic metal exposure on different population sizes have also been addressed. To do this, several environment route/receptor pathways have been considered in the risk assessment procedure. Multiple environmental pollution indices (e.g., CF and EF), parametric multivariate statistical model (PCA) and composite health risk assessment models (ADD_{der}, ADD_{inh}, ADD_{ing}, HQ, HI, and LCR) have been integrated. It is expected that findings from this research will provide baseline data on geochemical and health risk assessment for adequate environmental management and sustainability.

Fig. 1 a-b Artisanal mine activities, indiscriminate mine waste disposal activities, and human risk exposure to contaminants within the mine area

DESCRIPTION OF THE STUDY AREA

Location, climate, topography and relief

The studied area lies within the middle belt region of Nigeria occurring within Longitude 6°0′ 0″E and 6°12′0″E, and latitude 10°0′0″N and 10°8′0″N latitude of the Greenwich meridian. Topographically, the area is characterized by undulating high land and occasional lowlands, with the highest elevation reaching heights of 300.4m while low lands fall within an elevation of 177.9m (Fig. 2a). The area is characterized by two major seasons; a dry season which spans from November to April with very low humidity accompanied by the North-East trade winds characterized by harmattan periods. Maximum temperature conditions occur between 30°C and 36°C; recorded between December and Mid-January. The rainy season spans from April to November; characterized by high humidity and excessive heat. The average annual rainfall is between 150-250mm and usually; with peaks occurring between July and September. The vegetation in this area is typically that of the guinea savannah which is characterized by shrubs and very tall grasses with scattered trees of different species such as mango, cashews, etc. which are of economic importance. Asides from artisanal mining, animal husbandry (e.g., nomadic cattle rearing,) and subsistent agricultural activities (e.g., cultivation of perennial crops like yam, rice, millet, guinea corn, cowpea and groundnuts) make part of the occupation of the inhabitants.

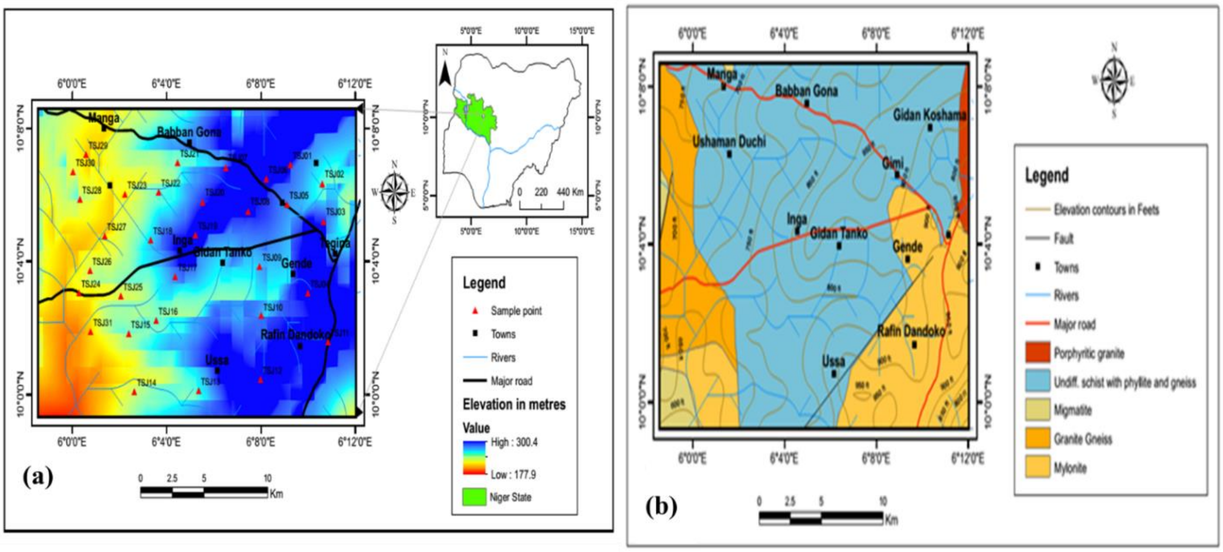

Fig. 2: Location and geologic map of the study area

GEOLOGY AND MINERALOGY

Geologically, the Tashan Jatau area occupies the central part of the Nigerian basement complex. The major lithostratigraphic framework of the area comprises metasedimentary and meta-igneous rocks which have undergone polyphase deformation and metamorphism similar to the basement rocks south east and south west of Nigeria (Okon et al., 2022; Omang et al.,2022). These rocks have been intruded on by granitic rocks of the Pan-African age. Five lithostratigraphic units have been recognized in the area- porphyritic granite, undifferentiated schist with phyllites and gneiss, migmatite, granite gneiss and masonite (Fig. 2b). The undifferentiated schist with phyllites and gneiss, which occurs, as a flat laying narrow southwest-northeast belt at the central part of Tashan Jatau with the gneiss occurring as small suites at the northern and southern part of the area forming contact with the granite. Feldspathic-rich pegmatite is bounded to the east, with an average width of 65meters and 100 meters long; with the pegmatite acting as the main host to the tourmaline mineralization. The area is dominated by granitic rocks with varying textures and compositions. Schists and phyllites, which are primarily found in the area's southwest and northeast, are the two main types of rocks that serve as host rocks for gold mineralization in the region.

MATERIALS AND METHODS

Sample collection and analyses

Homogenized surface soil samples (n=10) were taken systematically in duplicates using a hand trowel from hand-dug pits, trenches, and excavated areas where semi-mechanized mining and artisanal mining activities are ongoing. It should be noted however that the reason for fewer samples was because the current study was based on a preliminary investigation of the trace element geochemistry of the soil and mine tailings as well as the adverse health implication of human exposure. Sampling was done with a sample density of one sample every 50m-1km away from the mining site. This was done keeping in mind the fact that local artisanal miners may be exposed to toxic element ingestion, inhalation and dermal contact. Additionally, children around the area can be exposed to elemental ingestion and dermal contact through their playing habits. Moreover, crop plants grown around the area may take up these toxic elements through complex translocation and bioaccumulation processes within the soil-root system.

Approximately 3kg each of samples were collected to ensure that sufficient fined grained are retained for laboratory analyses. Two stages drying process was applied in drying the samples. To make the soil and sediment samples ready for sieving, they were air dried at room temperature. Samples were placed in plastic containers labelled with sample numbers and air dried in the laboratory. The second phase of drying was done on the sieved material in order to further expel moisture and make them suitable for final preparation and analysis. The samples were placed in disposable foil-type containers and oven-dried overnight at a temperature of about 50^{O}C. The dried samples were subsequently disaggregated by pressing a plastic gardener's scoop inside the containers. This was done in order to break lumps of soil, especially for those samples which were very wet when collected. It was followed by the removal of rock fragments, pebbles and organic debris from the samples prior to sieving. 2 mm and 63 µm stainless steel sieves were used to sieve the samples by closing the lid and manually shaking the assembly for about 3 minutes until all the fraction has been received in the pan. The finer fraction was then scooped from the receiving pan into clean, self-seal poly bags and labelled appropriately. Prior to analysis, the sieved test material was further dried overnight in an oven 100^{O}C. This was done to eliminate any moisture content. Between samples, the sieve pan, lid and scoop were thoroughly cleaned, first using a plastic brush, followed by wiping with clean, dry laboratory blue rolls.

GEOCHEMICAL ANALYSIS

Determination of total or near a total concentration of the trace elements and major oxides in soils and sediments was carried out by X-ray fluorescence (XRF) spectrometry method and Inductively Coupled Plasma Mass Spectrometry (ICP-MS).

X-ray fluorescence (XRF) spectrometry analysis

In order to determine total trace element concentration, pressed powder pellets were prepared. The procedure involved mixing 7.5 g of the sieved, oven-dried sample with three (3) cellulose tablets in a ratio of 1 cellulose tablet to 2.50 g of sample and grinding the mixture in an agate mill (Retsch RS 200) for 1 minute. This was followed by pressing the powder into 25 mm pellets using a hydraulic press at a pressure of 20 tons. The cellulose serves dual purposes as a binder and also reduces the absorption of the target material (Potts and Webb, 1992; Funtua, 2001). Glass beads were prepared for the determination of major constituents. This involved the mixing of approximately 7.60g of Lithium borate flux with 0.40g of the sample in a platinum crucible. The mixture was then fused on an air-acetylene flame (800 to 1200^{o}C) for fifteen (15) minutes so that the flux melted and the sample dissolves; the melt was placed in a one-phase glass bead to cool. Analysis was carried out using a high-performance sequential wavelength dispersive XRF spectrometer, S4 PIONEER from Bruker AXS, Germany. This was done using the default GEO-QUANT program for trace elements and the Beads-majors program for the major elemental constituents (oxides), with both running on the SPECTRA plus XRF software. The GEO-QUANT method provides quantitative analyses of a suite of 22 trace elements in a sample, with a typical analysis time of about 30 minutes per sample (Nehls and Ackland, 1973).

Inductively Coupled Plasma Mass Spectrometry(ICP-MS)

The soil samples were sieved through 10 mesh (2 mm), quartered, and pulverized in a porcelain mortar to 200 mesh (80 lm), re-homogenized and packaged in sealed plastic bags for chemical analyses. 0.25 g each of the powdered samples were digested by open vessel method using $HCLO_4$, HNO, and HF in a Teflon beaker placed on a hotplate put in a fume chamber, the mixture was then refluxed at a temperature of 90–100^oC for 1 h and then evaporated at a temperature ranging between 180^oC and 190^oC to dryness. A 5 ml volume of HCl was used to leach the residue. The digested samples were filtered through a 0.45 ml syringe membrane filter and made up to 10 ml with ultra-high purity water. The soil samples were analyzed for trace element concentrations at a certified commercial laboratory (Nigerian Geological Survey Agency, Kaduna) by inductively coupled plasma mass spectrometry (ICP-MS). The accuracy and precision of the analyses were assessed by introducing two blank samples, and two sample duplicates. The quality assurance and quality control (QA/QC) protocol was carried out and random duplicate samples were analyzed. Before and during the analysis, the instrument was calibrated to maintain accuracy.

DATA ANALYSIS

3.3.1 Quantitative assessment of soil pollution status

Multiple numerical soil pollution indices were integrated into the study for an in-depth analysis of the pollution level of the soils around the study area. To this end, complex numerical indices such as Contamination factor (CF) and enrichment factor (EF), were combined. Details on the definition of indices as well as an appropriate explanation of all indices have been provided in Table 1.

Model name	Equation(s)	Explanation and references	Soil pollution risk classification and reference
1. Enrichment factor (EF)	EF = (Cn/Cref) / (Bn/Bref)	Cn = content of the examined element in the examined environment C_{ref} = content of the examined element in the reference environment Bn = content of the reference element in the examine environment B_{ref} = content of the reference element in the reference environment (Simex and Helz 1981; Benhaddya and Hadjel 2013).	Background rank (EF ≤ 1); minimal enrichment (1< EF < 2); Moderate enrichment (2< EF <5); significant enrichment (5<EF <20); very high enrichment (20<EF<40); extremely high enrichment (EF >40) (Simex and Helz 1981; Benhaddya and Hadjel 2013;)
2. Contamination factor (CF)	$C^i_f = C^i/C_n$	$\mathbf{C^i_f}$=single-element contaminant factor; C^i = mean concentration of the element in samples at five locations; $\mathbf{C^i_n}$ = reference value for the element (concentration of an element on the earth's crust) (Taylor and McLennan 1985; Quinjie et al. 2008)	Low contamination (cf<1); Moderate contamination (1≤cf<3); Considerable contamination (3≤cf<6); High contamination (cf≥6) (Quinjie et al. 2008; Taylor and McLennan 1985)

MULTIVARIATE STATISTICS

Parametric numerical indices such as principal component analysis (PCA), was used for pollution source identification determination of the association between trace elements and oxides of analyzed soil samples. All analyses were conducted using the IBM SPSS (ver. 25.0). Significant correlations between analyzed parameters were taken at $p < 0.05$. Strong, moderate and weak loadings were considered at values = > ±0.75, 0.5-0.75, and <0.50 respectively for the PCA (Mustapha 2012).

HUMAN HEALTH RISK EVALUATION

Animal husbandry (e.g., nomadic cattle rearing) and subsistent agricultural activities (e.g. cultivation of perennial crops like yam, rice, millet, guinea corn, cowpea and groundnuts) constitute the major occupation of the inhabitants of the study area. mine wastes are improperly disposed of in stockpiles of mine spoils and tailings. Apparently, given the undulating topography, the mine spoils are washed downslope to nearby farmlands rivers and other water bodies, thereby constituting a contamination source. Moreover, during mining activities, the local miners are exposed to risk from toxic element ingestion, inhalation (through dust) and dermal contact. The children are not left out as their playing habits can take up toxic elements directly through ingestion or indirectly through dermal contact and inhalation. Therefore, they appear to be an adverse Consumers of fruits and crop plants from farmlands adjacent to the mine sites may be exposed to the risk of metal contamination directly through the feeding chain (through the consumption of vegetables, fruits and crops). The animals such as cattle can also be exposed to toxic metal ingestion through their feeding habits; thereby constituting a plant-animal-human pathway of toxic element contamination (Nganje et al. 2010; Omeka and Igwe 2021). This calls for an urgent holistic health risk assessment and monitoring for adequate environmental protection and human safety (Pavilonis et al. 2017; Lü et al. 2018; Jahromi et al. 2020). To achieve this, it will be important to identify the potential exposure to the hazards, the level of exposure of humans to the hazards, the likely effect of the hazard on the health of inhabitants and detailed characterization of the risk level (US-EPA multiple pollution risk pathway from mining activities within the area on the health of the inhabitants. 2017; Egbueri et al. 2020). To carry out the health risk assessment, two major probabilistic risk criteria were considered- the non-carcinogenic and carcinogenic risk indices. The non-carcinogenic risk considers the probability of human exposure to non-cancer-causing elements or pollutants, while the carcinogenic risk considers the likelihood of the exposure of humans to cancer-causing toxic elements in a particular environmental system (US-EPA 2017; Egbueri et al. 2020; Omeka et al. 2022a, b). The US-EPA (2017) risk assessment model was used in this study. Three pollution exposure pathways (ingestion, dermal contact and inhalation) were considered with two population sizes (children and adults) put into consideration. Details of all heavy metal indices as well as their parameters are given in Table 2 and 3.

Table 2 Numerical models for human health risks assessment of soils

Parameter	Equation	Equation definition and references
1. Daily exposure assessment	ADD_{ing} = Ci x R_{ing} x EF x ED ADD_{inh} = Ci x IRinh x EF x ED BW x AT PEF x BW x AT ADD_{derm} = Ci x SA x AF x ABS x EF x ED BW x AT	ADD_{der}, $ADD_{nh,}$ and $ADD_{ing,}$ (mg/kg/d) respectively refers to the average daily dose (ADD) of heavy metals through dermal contact, inhalation, and ingestion (mg/kg/d); IR_{inh} (mg/d) and IRi_{ng} (m3/d) represents the inhalation and ingestion rates of soil; Ci represents the concentration of each heavy metal in the soil; EF refers to the exposure frequency (day/year); SA represents the exposed surface area of skin (cm^2); ED is the exposure duration (year); ABS represents the dermal absorption factor; AF is the adherence factor (kg/m2/day); PEF refers to the particle emission factor (m^3/kg); BW refers to the body weight (kg); AT represents the average time (day) (US-EPA 2011, 2017).
2.Non-carcinogenic risk assessment	$HQ = ADD_{(inh,\ derm,\ ing);}\ HI = \sum^{HQ} = \sum^{ADD(ing,\ inh,\ derm)} /\ ^{RfD}$	RfD refers to the reference dose of a particular heavy metal (mg/kg/day). and is given as Zn (0.3), Sr (0.0015), V (0.009), Cr (0.003), Cu (0.04), Ba (0.07), and Pb (0.0035). HQ and HI represents the hazard quotient. hazard index respectively (Jia et al. 2018; US-EPA 1989, 2011; Egbueri et al. 2020) The HI and HQ based on inhalation (inh), ingestion (ing), and dermal contact (derm) were calculated for children and adult population. As per US-EPA (1989, 2011), non-carcinogenic risk can be categorized

		(by HI) into negligible risk (HI<0.1), low risk (HI=0.1-1), medium risk (HI=1-4), and high risk (HI>4).
3a Carcinogenic risk (CR) assessment	$\sum \text{ADD}_{\text{(ing, derm, inh)}}$ x CSF	CSF represents the cancer slope factor. CSF values for the carcinogens are: 0.0085 (Pb), 1.5 (As), 0.5 (Cr), 0.0015 (Sr) (IARC 2011; IRIS 2011; US-EPA 1989, 2011). CR based on inhalation (inh), ingestion (ing), and dermal contact (derm) calculated for children and adult population
3b. Lifetime cancer risk (LCR)	∑CR (inhalation + dermal + ingestion)	CR refers to the calculated cancer risk based on inhalation, ingestion, and dermal contact (Egbueri et al. 2020)

Table 3 Human health risk assessment parameters

Description		Value
a)	1. Skin area available for soil contact (SA)	5700 for adults and 2800 for children (in cm^2)
b)	2. Soil-to-skin adherence factor (AF)	1×10^{-6} for children; 2×10^{-7} for adults ($kg/cm^2/day$)
c)	3. Ingestion rate of soil (IR_{ing})	50 for children; 20 for adults (mg/day)
d)	4. Inhalation rate of soil (IR_{inh})	7.6 for children; 16 for adults (m_3/day)
e)	5. Dermal absorption factor (ABS)	0.001 (for all the heavy metals)
f)	6. Exposure frequency (EF)	350 (for both children and adults) (day/year)
g)	7. Exposure duration (ED)	6 for children; 24 for adults (year)
h)	8. Particle emission factor (PEF)	1.36×10^9 (m^3 kg)
i)	9. Body weight (BW)	29 for children; 65 for adults (kg)
j)	10. Average time (AT)	ED x 365 (day)
k)	11. Lifetime exposure expressed	76.5 x 365(day)
l)	in day (LT)	

RESULTS AND DISCUSSION

Geochemical characteristics of trace elements and oxides

Results of trace elements from XRF and ICP-MS analysis are given in Table 4, while descriptive statistical results of major oxides are presented in Table 5. Variation of trace elements and oxides is shown graphically in Fig. 3a and b respectively. The trace elements' results were compared with the average crustal values (Mason and Moore, 1982) and the Upper Continental Crust (UCC) (Rudnick and Gao 2014). As proposed by Adamu et al. (2021), mean trace element concentrations in soils > 50ppm is considered extremely high; 1-50 are considered medium, while those < 1 are categorized as depleted. Generally, extremely high elemental concentration was recorded in Vanadium (V), Copper, Chromium (Sr), Zirconium (Zr), Barium (Ba), Zink (Zn), Lead (Pb), and Talium (Ta). Medium trace elemental concentration was recorded for Cerium (Ce), Gnome (Gn), Arsenic (As), Rubidium (Rb), Yttrium (Y), Niobium (Nb), Tungsten (W), Hafnium (Hf), Tin (Sn), and antimony (Sb). Only Scandium (Sc) occurred in depleted concentration among the soil samples. When compared with the average crustal values of Mason and Moore (1982), all the soil samples recorded concentrations above the crustal values for V, Cr, Cu, Sr, Zr, and Pb. However, 40% of the soil samples (TSJ 1, TSJ 5, TSJ 7, TSJ 8), recorded concentration within the average crustal value for Zn, while a greater percentage of the samples (TSJ 2, TSJ 3, TSJ 4, TSJ 6, TSJ 9, TSJ 10), recorded relatively high Zn concentration to that of the average crustal value. In mineralized soils, Zn is said to be highly immobile with high depletion occurring in surface soil relative to the subsurface geologic material (Olade 1976); hence its concentration is expected to increase with depth. The high concentration in the soil can be therefore attributed to anthropogenic activities such as mining. The extremely high concentration of V, Cr, Sr, Zr, and Pb in the surface soil reflects their relatively low mobility potential within the soil system (Olade 1976). Moreover, these groups of metals have a strong tendency to form metallo-organic complexes with soil organic matter within surface soils (Nganje et al. 2021). Moreover, the probable source of Cr could be from geochemical processes such as chemical weathering of igneous and ultramafic rocks (Nganje et al. 2021). Porphyritic granite, undifferentiated schist with phyllites and gneiss are said to constitute the bedrock lithology of the area. Weathering and possible oxidation of exposed mine spoils may have elevated their concentration in the soil. All the soil samples, (except for TSJ 8), recorded Pb concentration above the Average crustal value. Pb concentration in soil is often associated with the chemical weathering of the shale from sulphide ores (e.g., galena (PbS)

When compared with the trace elements of the UCC, all the soil samples recorded relatively higher concentrations for Cr, Sr, Rb, Sb, Ta and Zr. The higher variation in concentration was however recorded for Ba and Sc across all the soil samples; 20% of the soil samples (TSJ 3 and TSJ 8) recorded Ba values within those obtained from the UCC (Rudnick and Gao 2014), while 80% recorded higher values. However, the concentration of Sc was within that of the UCC (Table 4). These results seem to agree with those of Adamu et al. (2020) on the geochemistry of trace elements in grey and black shales within the Calabar Flank, Southeastern Nigeria, where relatively lower values were recorded for Ba and Sc when compared to the UCC (Rudnick and Gao 2014). From the results of the present study, the high enrichment of trace elements in the soil above those of the UCC is a clear indication that asides geogenic (crustal) inputs, and anthropogenic processes, also play a vital role in their enrichment in the soil. This is in agreement with Jia et al. (2018).

Table 4 Descriptive statistics of the concentration of trace and potentially toxic elements (PTEs) in the Tashan Jatau mine district

												STANDARDS	
	TSJ 1	**TSJ 2**	**TSJ 3**	**TSJ 4**	**TSJ 5**	**TSJ 6**	**TSJ 7**	**TSJ 8**	**TSJ 9**	**TSJ 10**	**Mean**	**Variance**	**A**	**B**
V	720	520	399	501.01	283	398.06	400	502	254	518	449.507	254-720	130	
Cr	212.02	677	220	318.02	614.2	710.1	530.19	425	648.29	945	529.982	212.02-710.1	90	92
Cu	425	360	350	480	379	460	340	290	330	330	374.4	290-480	45	
Sr	2230	493	2050	1890	980	1020	1450	290	1220	2030	1365.3	493-2230	300	320
Zr	1600	2700	4310	5720	940	7340	1000	720	1200	1500	2703	720-7340	160	193
Ba	690	8400	200	680	700	1030	900	100	3100	1800	1760	100-8400		624
Zn	58	190	380	100	60	1300	30	50	97	560	282.5	30-1300	95	
Ce	58.03	39.88	50	30	44	77	42	45	50	54	48.991	30-77		
Pb	84	31	92	75	9.09	47	25	17	26	867	127.309	17-867	20	
Gn	26	9	24	34.02	19.9	31	22	17.4	39	22	24.432	9.0-34.0	-	
As	15.05	6	9	22	11	4	15	7	7.02	17	11.307	04-15.05	-	
Y	2.9	20	28	10	28	87	15	39	15	3.9	24.88	2.9-87	-	
Rb	39	86	17	21.6	5.5	13	30	9.84	29	30	28.094	5.5-86	-	84
Nb	18.001	20.1	76	15	40.03	11	48	14	32.01	83	35.7141	11.0-76.0		
Ta	41.2	64.09	81	70.2	61	40.24	36	64	42.1	64	56.383	36-70.2	-	0.9
W	0.882	3.99	4.34	12	6.066	12.3	0.96	13.3	0.891	1.46	5.6189	0.82-13.3	-	
Hf	11	14	51	39.45	20.4	18.09	20	16	33	21	24.394	11.0-51.0	-	
Sn	43.4	47.23	39.12	61.22	48.23	40.55	17.03	9.88	31.06	20.12	35.784	9.88-61.22	-	
Sb	3.24	0.5	7	8.01	4.04	10	6.13	12	7.03	14	7.175	0.3-14		0.4
Sc	<0.001	0.25	0.034	0.2	0.2	0.1	0.21	0.28	<0.001	0.012	0.1286	0.001-0.28		14.0

A-Average crustal values (Mason and Moore, 1982); B-Upper Continental Crust (Rudnick and Gao 2014)

The concentration of major oxides decreased in the order SiO_2 > Fe_2O_3 > Al_2O_3 > K_2O > TiO_2 > CaO (Table 5; Fig. 3b). SiO_2 had a mean concentration of 39.306% varying between 19.85 and 60.07%; Fe_2O_3 ranged from 16.77-52.95%, with a mean value of 33.446; Al_2O_3 recorded a mean of 11.055% ranging from 5.24 -18.07% (Table 5). Oxides such as K_2O, TiO_2 and CaO showed average mean values of 3.22%, 2.765% and 1.334% respectively. The rest of the oxides recorded lower mean values; indicating lesser concentration in the study area. The variation of the major oxides distribution chart (Fig 3b) revealed that SiO_2, Fe_2O_3 and Al_2O_3 are highly enriched in all the samples however, CaO, K_2O, and TiO_2 showed a moderate enrichment pattern in the samples. Furthermore, MgO was observed to be depleted in all the studied samples except for TSJ 6 which is moderately enriched. Although, SO_2, MnO, P_2O_5 and Cl also revealed depletion while LOI is averagely enriched.

(a) (b)

Fig. 3 a-b Graphical distribution of trace elements and oxides in the soil samples

Table 5 Major oxides concentration of the Tashan Jatau mine district

	TSJ 1	TSJ 2	TSJ3	TSJ 4	TSJ 5	TSJ 6	TSJ 7	TSJ 8	TSJ19	TSJ10	MEAN	RANGE	SD
SiO_2	40.45	29.79	54.92	57.86	32.25	24.47	50.28	23.12	19.85	60.07	39.306	19.85-60.07	14.635
CaO	1.27	1.47	1.37	1.43	1.46	1.08	1.27	1.66	1.36	0.97	1.334	0.97-1.66	0.189
MgO	0.86	0.75	0.56	0.64	0.79	1.66	0.72	0.52	0.29	0.58	0.737	0.29-1.66	0.344
SO_2	0.32	0.46	0.79	1.28	0.47	0.27	0.87	0.72	0.41	0.64	0.623	0.27-1.28	0.290
K_2O	5.61	2.48	3.02	3.15	4.05	4.29	2.12	3.25	1.48	2.75	3.22	1.48-5.61	1.122
Na_2O	0.33	0.23	0.22	0.17	0.13	0.36	0.18	0.16	0.22	0.17	0.217	0.13-0.36	0.071
TiO_2	2.79	2.91	1.39	1.58	2.79	2.8	4.23	2.65	3.4	3.11	2.765	1.39-3.4	0.775
MnO	0.04	0.06	0.08	0.11	0.08	0.1	0.05	0.1	0.07	0.08	0.077	0.04-0.11	0.022
P_2O_5	0.88	0.25	0.2	0.31	0.24	0.19	0.14	0.47	0.28	0.12	0.308	0.12-0.88	0.212
Cl	0.06	0.9	0.63	0.22	0.16	0.5	0.18	0.83	0.8	0.85	0.513	0.06-0.9	0.314
Fe_2O_3	23.25	41.92	24.88	17.49	33.33	49.43	27.2	47.34	52.95	16.77	33.446	16.77-52.95	12.845
Al_2O_3	18.07	12.19	5.24	7.74	17.42	10.71	5.9	13.14	14.24	5.9	11.055	5.24-18.07	4.512
LOI	6.06	6.57	6.6	8.01	6.94	4.16	6.86	6.03	4.67	7.98	6.388	4.16-8.01	1.180

Trace element source identification and elemental association

The unrotated principal analysis scores of trace elements and oxides are presented in Table 6. Data was statistically normalized following the Kaiser (1960) normalization criterion; with only factor classes with eigenvalues ≥1 considered significant. A total of nine principal components were extracted, accounting for 100% of the overall data variance. PC1 accounted for a variance of 22.321% showing positive significant loadings for trace elements (Ce, Y) and oxides (MgO, Na_2O, Fe_2O_3 and Al_2O_3). A significant negative loading was observed among trace elements (Sr, Nb, As, Ta, Hf) and oxides (SiO_2, and SO_2). The significant positive loading observed for the two lanthanide elements (Ce and Y) can be associated with similarity in physicochemical characteristics. Lanthanide elements are characteristically electronegative, have similar ionic radii, and exist in the 3^+ electron valency (Migaszewski and Gałuszka 2015). Moreover, lanthanides tend to occur together in the soil phase rather than as single elements (Tyler 2004). The strong negative loading observed for Sr, Nb, Ta, Hf suggests that they occurred from a similar environmental condition. According to the Goldschmidt classification (1937), these elements are lithophilic; highly reactive metals of the f- and s-blocks with a high affinity for oxygen. Hence they have a high propensity to be bounded to the surface soils. The strong significant positive loading observed between SiO_2, Fe_2O_3 and Al_2O_3 revealed the prevalence of quartz and clay minerals in the study area. This could be sourced from bedrock lithology. The strong positive significant loading observed for Fe_2O_3 and MgO among this component class suggests that the elements that constitute these oxides may have originated through erosion, leaching and other related weathering activities of igneous and ultramafic rocks that constitute the subsurface geology.

PC2 explained 18.91% of the variance with positive significant loadings for Cu, Zr, Zn, MgO, K_2O, and MnO. The occurrence of these trace elements in this component class can be traced to anthropogenic and geogenic sources. The occurrence of Cu and Zn can be traced to their similarity in geochemical behaviour (chalcophile). Surface environmental conditions such as oxidation, leaching and weathering may have given rise to the occurrence of the oxides (such as K_2O, and MnO). PC3 (with 16.295% of the total variance) had a relatively significant positive loading for potentially toxic elements (PTEs) such as Cr, Zn and Sb. Apparently, Cr and Zn have a comparable anthropogenic source of occurrence in surface soils most likely from the ongoing mining activities in the area. The occurrence of Sb in the soil can be attributed to lithospheric sources from the underlying parent material. The strong positive loading observed for the transition trace elements (V, Cr, Zn), could be attributed to similarity in geochemical properties including similarity in radius and size. PC4 (having 14.283% of the overall variance) showed high positive loadings for Sr, Pb, and Ce. It is therefore critical to emphasize that the robust nexus exhibited between PTEs in this component class can be traced to similar environmental and pollution sources such as poor mine waste disposal. The strong positive loading observed in PC5 for Ba, and Rb (0.777 and 0.752 respectively), can be attributed to high-pressure acidic gneisses complexes which make up the geology of the study area. PC6 showed a significant positive loading for V and a negative significant loading for Gn. The negative loading observed for Gn can be attributed to its occurrence from a different source.

Table 6 Results of the Kaiser unrotated Principal Components analysis (PCA) of trace elements, oxides and PTEs

Parameters	1	2	3	4	5	6	7	8	9
V	-0.083	0.157	**0.561**	0.307	0.162	**0.646**	0.027	0.266	-0.209
Cr	0.203	-0.321	**0.626**	0.403	0.178	0.022	-0.357	0.034	0.376
Cu	0.193	**0.791**	-0.366	0.014	0.266	-0.182	-0.272	0.083	0.134
Sr	**-0.569**	0.493	-0.25	**0.517**	-0.043	-0.185	0.251	0.068	0.024
Nb	**-0.636**	-0.098	0.419	0.422	0.034	-0.051	0.314	-0.359	0.048
Zr	0.231	**0.815**	0.189	-0.133	0.436	-0.118	-0.017	0.087	-0.137
Ba	0.213	**-0.559**	-0.029	0.024	**0.777**	-0.048	-0.063	0.157	0.079
Zn	0.488	**0.545**	**0.545**	0.333	0.219	0.066	0.045	-0.042	-0.022
Ce	**0.659**	0.336	0.24	**0.528**	-0.148	0.046	0.299	-0.044	-0.011
Pb	-0.433	0.029	0.402	**0.634**	0.078	0.374	0.265	0.138	0.303
Gn	0.003	0.491	0.072	0.037	-0.329	**-0.597**	0.102	**-0.502**	0.156
As	**-0.755**	0.299	-0.326	0.202	-0.098	0.028	-0.383	0.158	0.104
Y	**0.742**	0.38	0.442	-0.197	-0.024	0.042	-0.021	-0.209	-0.16
Rb	0.054	-0.483	-0.301	0.211	**0.752**	0.046	-0.036	0.203	-0.136
Ta	**-0.533**	0.133	0.189	-0.479	0.357	0.382	0.303	-0.185	0.183
W	0.289	0.495	0.225	**-0.645**	-0.059	0.364	-0.246	0.083	-0.034
Hf	**-0.541**	0.364	0.267	-0.355	0.101	-0.436	0.418	0.023	-0.043
Sn	0.029	0.476	-0.449	-0.242	**0.534**	-0.277	-0.039	-0.074	0.379
Sb	-0.168	0.292	**0.691**	0.119	-0.433	0.343	-0.028	0.299	0.011
SiO_2	**-0.839**	0.367	-0.025	0.305	0.152	0.078	-0.085	-0.118	-0.135
CaO	-0.015	-0.343	-0.298	**-0.874**	-0.085	0.109	0.065	-0.042	-0.077
MgO	**0.677**	**0.553**	0.028	0.242	0.154	0.076	-0.262	-0.262	-0.111
SO_2	**-0.767**	0.245	0.06	-0.404	0.008	0.005	-0.311	0.128	-0.266
K_2O	0.344	**0.526**	-0.546	0.168	-0.172	0.393	0.084	-0.248	0.162
Na_2O	**0.658**	0.395	-0.228	0.397	0.182	-0.071	0.282	0.186	-0.231
TiO_2	0.253	**-0.607**	0.07	0.496	-0.267	-0.215	-0.423	0.023	-0.141
MnO	-0.001	**0.517**	**0.538**	**-0.554**	-0.043	0.213	-0.145	0.161	0.204
P_2O_5	0.193	0.048	**-0.805**	0.024	-0.281	0.303	0.263	0.267	0.011
Cl	0.088	-0.433	**0.635**	-0.089	0.317	0.272	0.341	0.321	0.025
Fe_2O_3	**0.787**	-0.351	0.28	-0.333	-0.081	-0.159	0.111	0.162	-0.022
Al_2O_3	**0.554**	-0.246	**-0.561**	-0.131	-0.248	0.043	0.085	-0.004	0.479
Total	**6.921**	**5.862**	**5.051**	**4.428**	**2.734**	**2.141**	**1.616**	**1.188**	**1.061**
% of Variance	**22.321**	**18.91**	**16.295**	**14.283**	**8.819**	**6.907**	**5.212**	**3.831**	**3.421**
Cumulative %	**22.321**	**41.231**	**57.526**	**71.809**	**80.629**	**87.536**	**92.748**	**96.579**	**100**

Quantitative assessment of soil pollution status

Contamination factor and enrichment factor

Summary results of Cf and Ef are presented in Table 7. The EF is used to assess the anomalous concentration of trace elements in the soil by geochemically normalizing or standardizing the concentration of a particular element as a ratio to another element (normalizer or reference element) which serves as the background or baseline value of the element in soil with respect to the studied environment or area (Zhang et al. 2007). Trace elements such as Zr, Mn, K, Sr, Al, Sc, Fe, Zn, and Ti, have been used as reference elements by several studies (Zhang et al., 2007; Akoto et al., 2008; Nganje et al. 2020; Omeka et al. 2020a). In the present study, Sr was used as a reference or normalizer element. CF on the other hand used to evaluate the level of pollution from a given element in the surface soil, given as a ratio of the average value of at least five soil samples over the crustal value (reference value) of the element (Taylor and McLennan 1985; Mason and Moore 1982; Quinjie et al., 2008); Sr was chosen as the reference value for this study based on Taylor and McLennan 1985 criterion.

Results of EF showed that, apart from Cr, V, Zr, Ta, and Sr, all other analyzed trace elements demonstrated enrichment within the background range (EF ≤ 1). The enrichment of Cr ranged from moderate (2< EF <5) to significant (5<EF <20) enrichment in the soil media. 60% of the total samples (TSJ 1, TSJ 3, TSJ 4, TSJ 7, TSJ 9, TSJ 10) recorded moderate Cr enrichment in the soil, while 40% of the samples (TSJ 2, TSJ 5, TSJ 6, TSJ 8) recorded significant Cr enrichment. V enrichment ranged from moderate to extremely high (EF > 40) enrichment; with 50% of the samples (TSJ 3, TSJ 4, TSJ 7, TSJ 9, TSJ 10) showing significant V enrichment while 50% (TSJ 1, TSJ 2, TSJ 5, TSJ 6, TSJ 8) showed extremely high enrichment. The enrichment of Zr ranged from moderate to very high (20<EF<40) enrichment. 50% of the total samples (TSJ 1, TSJ 5, TSJ 7, TSJ 9, TSJ 10) recorded moderate Zr enrichment, while 40% of the samples recorded significant Zr enrichment. Very high enrichment was recorded in only one sample (TSJ 6). Ta enrichment in the soil ranged from background enrichment to significant enrichment. Only 20% of the samples (TSJ 1. TSJ 7) recorded enrichment within the background range for Ta, and 80% of the total samples (TSJ 2, TSJ 3, TSJ 4, TSJ 5, TSJ 6, TSJ 8, TSJ 9, TSJ 10) however occurred within the moderate enrichment range. Sr enrichment in the soil ranged from background to moderate enrichment, with 30% of the samples recording background enrichment for Sr, while 70% recorded moderate enrichment (Table 2). According to the Simex and Helz, (1981) Ef classification criteria, EF ranging from 0.5 to 1.5 indicates natural or crustal origin, while those above 1.5 are indicative of anthropogenic inputs. Confusion on the right classification criteria however arises in that if the enrichment of an element in the soil is greater than the background value (EF> 1), its source may be associated with both natural and anthropogenic inputs. To this end, some authors have agreed that the enrichment of trace elements in the soil is often times influenced by chemical alteration of the parent material giving rise to significantly high values sometimes exceeding the threshold or background value (Nganje et al., 2021; Omeka et al. 2022a). Hence to make up for this discrepancy in classification, an EF value of < 2 has been assigned to depict the anthropogenic source. Therefore, Cr, V, Zr, Ta, and Sr enrichment can be attributed to anthropogenic sources, while Ba, Zn, Pb, As, Y, Nb, Hf, Sn, Sb, and Sc enrichment was from the parent material. These results have therefore shown that apart from mining activities in the area, trace elemental enrichment in the soil is also attributed to crustal sources.

The summary result of the contamination factor of all trace elements is presented in Table 7b. From the results, all analyzed soil samples recorded low CF values (cf<1) for Sb, Sc, and Hf; 90% of the soil samples recorded low CF values for Y while moderate CF (1≤cf<3) was reported in one sample (TSJ 11). 80% of the soil samples recorded low CF values for Ba while 20% (TSJ 2 and TSJ 9) recorded moderate CF values. 100% of the soil samples recorded high contamination (CF > 6) for Cr, V, Cu, Zr, and Ta. 80% of the samples recorded high contamination for Sr, while TSJ 2 and TSJ 9 recorded considerable and moderate contamination respectively with respect to Sr. 90% of the samples recorded low contamination for Pb; although high contamination was recorded in one sample (TSJ 10). High variability of contamination was observed for Zn and Sn- 60% of the samples (TSJ 1, TSJ 4, TSJ 5, TSJ 7, TSJ 8, TSJ 9) recorded low contamination with respect to Zn, and considerable contamination was recorded in two samples (TSJ 3, TSJ 10), while moderate and high Zn contamination was recorded in TSJ 2 and TSJ 6 respectively. Similarly, moderate contamination was reported in 50% of the total samples (TSJ 3, TSJ 6, TSJ 7, TSJ 9. TSJ 10) for Sn, while 40% of the samples (TSJ 1, TSJ 2, TSJ 4, TSJ 5) recorded considerable contamination. Only one sample (TSJ 8) recorded low contamination for Sn. Moderate contamination was recorded in all the soil samples with respect to Arsenic (As).

Results from both EF and CF have shown that the enrichment of toxic trace elements in the soil within the area is influenced by Cr, V, Cu, Zr, Sr and Ta enrichment. Although mining activities seem to play a major role in the distribution and availability of these elements in the soil, crustal (geogenic) sources also influence their enrichment.

Table 7 Results of enrichment factor EF and contamination factor CF trace elements concentration of soil

(a) EF

Sample code	EF(Cr)	EF (V)	EF(Cu)	EF(Zr)	EF(Ba)	EF(Zn)	EF(Pb)	EF(As)	EF(Y)	EF(Rb)	EF(Nb)	EF(Ta)	EF(Hf)	EF(Sn)	EF(Sb)	EF(Sc)	EF(Sr)	Index	Range	Class
TSJ 1	1.21	22.6	13.3	2.23	0.0160	0.0331	0.0527	0.236	0.0455	0.0175	0.0565	0.718	0.00987	0.202	0.0678	2.09E-06	1.23	EF	EF ≤ 1	Background
																			2< EF <5	Moderate
TSJ 2	17.5	73.8	51.1	17.0	0.888	0.491	0.0880	0.426	0.142	0.174	0.285	5.06	0.0568	0.993	0.0028	0.0237	1.537		5<EF <20	Significant
TSJ 3	1.37	13.6	12.0	6.54	0.0050	0.236	0.0628	0.154	0.0478	0.00829	0.260	1.54	0.0498	0.198	0.0015	7.74E-05	1.54		20<EF<40	Very high
TSJ 4	2.14	18.6	17.8	9.42	0.0187	0.0673	0.0556	0.407	0.0185	0.0114	0.0556	1.44	0.0417	0.336	0.0019	0.00494	0.839		EF >40	Extremely high
TSJ 5	7.98	20.2	27.1	2.98	0.0370	0.0779	0.0130	0.393	0.101	0.00561	0.286	2.42	0.0416	0.510	0.0192	0.00952	0.718			
TSJ 6	8.86	27.3	31.6	22.4	0.0524	1.62	0.0645	0.137	0.299	0.0127	0.0755	1.53	0.0355	0.412	0.0458	0.00458	1.23			
TSJ 7	4.65	19.3	16.4	2.15	0.0322	0.0263	0.0241	0.362	0.0362	0.0207	0.232	0.966	0.0276	0.122	0.0197	0.00676	0.939			
TSJ 8	18.7	121	70.0	7.72	0.0179	0.219	0.0821	0.845	0.471	0.0339	0.338	8.58	0.110	0.353	0.0193	0.00451	1.84			
TSJ 9	6.76	14.6	18.9	3.06	0.132	0.101	0.0298	0.201	0.0430	0.0238	0.184	1.34	0.0541	0.264	0.0269	3.83E-06	2.84			
TSJ 10	5.92	17.9	11.4	2.30	0.0460	0.351	0.598	0.29	0.00672	0.0148	0.286	1.23	0.0207	0.103	0.0322	2.76E-05	1.84			

(b) CF

Sample code	CF(Cr)	CF (V)	CF(Cu)	CF(Sr)	CF(Zr)	CF(Ba)	CF(Zn)	CF(Pb)	CF(As)	CF(Y)	CF(Rb)	CF(Nb)	CF(Ta)	CF(Hf)	CF(Sn)	CF(Sb)	CF(Sc)	CF	(cf<1)	Low
TSJ 1	19.3	360	213	15.9	35.6	0.256	0.527	0.840	3.76	0.0725	0.279	0.900	11.4	0.157	3.21	0.0108	3.33E-05		(1≤cf<3)	Moderate
TSJ 2	61.5	260	180	3.52	60.0	3.11	1.73	0.310	1.50	0.500	0.614	1.01	17.8	0.20	3.50	0.00100	0.0833		(3≤cf<6)	Considerable
TSJ 3	20.0	200	175	14.6	95.8	0.0741	3.45	0.920	2.25	0.70	0.121	3.80	22.5	0.729	2.90	0.0233	0.0113		(cf≥6)	High
TSJ 4	28.9	251	240	13.5	127	0.252	0.909	0.750	5.50	0.250	0.154	0.750	19.5	0.564	4.53	0.0267	0.0667			
TSJ 5	55.8	142	190	7.00	20.9	0.259	0.545	0.090	2.75	0.70	0.0393	2.00	16.9	0.291	3.57	0.0135	0.0667			
TSJ 6	64.6	199	230	7.29	163	0.381	11.8	0.470	1.00	2.18	0.0929	0.550	11.2	0.258	3.00	0.0333	0.0333			
TSJ 7	48.2	200	170	10.4	22.2	0.333	0.273	0.250	3.75	0.375	0.214	2.40	10.0	0.286	1.26	0.0204	0.0700			
TSJ 8	38.6	251	145	2.07	16.0	0.0370	0.455	0.170	1.75	0.975	0.0703	0.700	17.8	0.229	0.732	0.0400	0.0933			
TSJ 9	58.9	127	165	8.71	26.7	1.15	0.882	0.260	1.76	0.375	0.207	1.60	11.7	0.471	2.30	0.0234	3.33E-05			
TSJ 10	85.9	259	165	14.5	33.3	0.667	5.09	8.67	4.25	0.0975	0.214	4.15	17.8	0.300	1.49	0.0467	0.0040			

Human health risk evaluation

Daily dose exposure assessment

Daily dose risk assessment of the exposure to contaminants was calculated for three exposure pathways- inhalation (ADD_{inh}), ingestion (ADD_{ing}), and dermal contact (ADD_{der}), with emphasis on the children and adult population within the study area. For the daily dose exposure assessment, nine potentially toxic elements (PTEs) (Pb, As, Cr, Sr, Ba, Zn, V, Cu) were considered. As observed in Table 8a, the risk ranking in terms of exposure pathways decreased in the order of $ADD_{der} > ADD_{ing} > ADD_{inh}$ for the adult population, while for the children population, ranking occurred in the order of $ADD_{ing} > ADD_{der} > ADD_{inh}$. The implication of this result is that local artisanal miners are at a very high risk of exposure to these contaminants through their skin during mining activities. Meanwhile, children around the mining area will be more exposed to these toxic elements when they ingest them. Generally, higher risk values were observed for the children population for all exposure routes; this is due to the lower body weights of the children compared to adults.

Table 8 (a) Results of average daily dose exposure assessment (b) Results of non-carcinogenic risk (hazard index) assessment of soils

(a)

Sample ID	Adult population ADD_{ing}	ADD_{derm}	ADD_{inh}	Children population ADD_{ing}	ADD_{derm}	ADD_{inh}
TSJ 1	0.0133229	0.093126235	9.75E-12	0.584632	0.467361	8.5E-11
TSJ 2	0.024287	0.104090285	1.78E-11	1.059741	0.565659	1.57E-10
TSJ 4	0.0120337	0.091837035	8.81E-12	0.528767	0.455802	7.65E-11
TSJ 5	0.0126766	0.09247987	9.28E-12	0.556623	0.461566	8.08E-11
TSJ 7	0.0108681	0.090671405	7.95E-12	0.478256	0.445352	6.88E-11
TSJ 11	0.0142627	0.094065978	1.04E-11	0.625355	0.475786	9.12E-11
TSJ 12	0.0120165	0.091819807	8.79E-12	0.528021	0.455648	7.64E-11
TSJ 13	0.0084879	0.088291198	1.18E-11	0.375114	0.424012	9.95E-11
TSJ 14	0.0155151	0.095318437	1.14E-11	0.679628	0.397544	1.15E-10
TSJ 15	0.017947	0.097750277	1.32E-11	0.785008	0.054889	1.25E-10

(b)

	Adult population			Children population		
Sample ID	Hi_{ing}	Hi_{derm}	Hi_{inh}	Hi_{ing}	Hi_{derm}	Hi_{inh}
TSJ 1	6.344672616	53.95511	4.6405E-09	279.2945145	264.4477025	4.01461E-08
TSJ 2	4.655911542	52.26635	3.3988E-09	206.114868	249.307086	2.90133E-08
TSJ 3	6.030852303	53.64129	4.4098E-09	265.6956343	261.6341411	3.80773E-08
TSJ 4	6.004493173	53.61493	4.3904E-09	264.5534053	261.3978179	3.79035E-08
TSJ 5	4.968254944	52.57869	3.6285E-09	219.6497487	252.1074062	2.14938E-10
TSJ 6	5.090819911	52.70126	3.7186E-09	224.9608973	253.2062645	3.18803E-08
TSJ 7	5.526722086	53.13716	4.0391E-09	243.8499915	257.1143529	3.47539E-08
TSJ 8	4.053895217	51.66433	9.7056E-09	180.0274939	243.9096983	3.33056E-08
TSJ 9	5.307014903	52.91745	3.8776E-09	234.329347	237.1735387	4.40121E-08
TSJ 10	6.931112115	54.54155	5.0718E-09	304.7068928	269.705436	3.40E-08
Min	4.053895217	51.66433	3.3988E-09	180.0274939	237.1735387	2.14938E-10
Max	6.931112115	54.54155	9.7056E-09	304.7068928	269.705436	4.40121E-08
Mean	5.491374881	53.10181	4.6881E-09	242.3182793	255.0003444	3.23319E-08

Non-carcinogenic health risk evaluation

The non-carcinogenic risk assessment was carried out using hazard quotient (HQ) and hazard index (HI) coefficients. The HI results are presented in Table 7b, while overall HQ results are presented in Table 9-14. The occurrence of the trace elements in HQ for the three risk exposure pathways for both children and adults was observed to be in the following order: ingestion risk pathway (As > Sr > Cr > Pb > V > Ba > Cu > Zn); dermal contact risk pathway (As > Sr > Cr > Pb > V > Cu > Ba > Zn); inhalation risk pathway (As > Sr > Cr > Pb > V > Ba > Cu > Zn). Meanwhile, based on the various exposure routes, the HQs for both population sizes occurred as $HQ_{ing} > HQ_{der} > HQ_{inh}$ (Table S2-S7). Based on the HI risk classification criteria (US-EPA 2017), it is observed that all the soil samples within the area expose the children and adults within the vicinity of the mine area to very high chronic risks ($HI \geq 4$) due to ingestion and dermal contact; with higher risk levels observed for the children population than adults. A negligible cancer risk (≥ 0.1 $HI < 1$) based on inhalation, was however recorded for both populations. These results seem to agree with those of previous studies in the southeastern and southwestern regions of Nigeria (Omeka et al. 2022a and Egbueri et al. 2020) on the health risk assessment of toxic elements in soil in mining areas. Results of the present study imply that inhabitants within the vicinity of the district of the Tashan Jatau mine are exposed to higher chronic risk levels from ingestion and dermal contact than inhalation from soils within the mining area.

Table 9 Overall Hazard quotients (HQ_{ing}) results of adult's population for the ingestion pathway

Sample ID	HQ (Pb)	HQ (As)	HQ (Cr)	HQ (Sr)	HQ (Ba)	HQ (zn)	HQ (V)	HQ (Cu)
TSJ 1	0.23985147	2.394626	0.354771	3.07224	0.027197	0.002646	0.217383	0.035959
TSJ 2	0.21325706	2.341646	0.626976	1.03852	0.220633	0.003419	0.178355	0.033105
TSJ 3	0.24386572	2.359209	0.359443	2.861492	0.014903	0.004531	0.154744	0.032666
TSJ 4	0.23533544	2.435312	0.416825	2.67416	0.026946	0.002892	0.17465	0.038374
TSJ 5	0.20226303	2.370917	0.590212	1.608711	0.027447	0.002658	0.132108	0.033939
TSJ 6	0.22128556	2.329938	0.646353	1.655544	0.035727	0.009917	0.15456	0.037496
TSJ 7	0.21024637	2.394333	0.541031	2.158998	0.032465	0.002482	0.154939	0.032227
TSJ 8	0.20623212	2.3475	0.479452	0.800843	0.012394	0.002599	0.174843	0.030032
TSJ 9	0.21074816	2.347617	0.610169	1.889708	0.087661	0.002874	0.126449	0.031788
TSJ 10	0.63274625	2.406041	0.783866	2.838075	0.055045	0.005585	0.177965	0.031788
Min	0.20226303	2.329938	0.354771	0.800843	0.012394	0.002482	0.126449	0.030032
Max	0.63274625	2.435312	0.783866	3.07224	0.220633	0.009917	0.217383	0.038374
Mean	0.26158312	2.372714	0.54091	2.059829	0.054042	0.00396	0.1646	0.033737

Table 10 Overall Hazard quotients (HQ_{derm}) results of adult's population for dermal contact pathway

Sample ID	HQ (Pb)	HQ (As)	HQ (Cr)	HQ (Sr)	HQ (Ba)	HQ (zn)	HQ (V)	HQ (Cu)
TSJ 1	3.08996989	35.64601	3.679909	9.722516	0.169702	0.035897	1.325762	0.285344
TSJ 2	3.06337548	35.59303	3.952114	7.688796	0.363139	0.03667	1.286735	0.28249
TSJ 3	3.09398414	35.61059	3.684581	9.511768	0.157409	0.037782	1.263123	0.282051
TSJ 4	3.08545386	35.68669	3.741963	9.324436	0.169452	0.036143	1.283029	0.287759
TSJ 5	3.05238145	35.6223	3.91535	8.258987	0.169953	0.035909	1.240487	0.283325
TSJ 6	3.07140398	35.58132	3.971491	8.30582	0.178233	0.043168	1.26294	0.286881
TSJ 7	3.0603648	35.64571	3.86617	8.809274	0.174971	0.035734	1.263318	0.281612
TSJ 8	3.05635054	35.59888	3.80459	7.451119	0.1549	0.035851	1.283222	0.279417
TSJ 9	3.06086658	35.599	3.935307	8.539985	0.230167	0.036126	1.234828	0.281173
TSJ 10	3.48286467	35.65742	4.109004	9.488351	0.197551	0.038836	1.286344	0.281173
Min	3.05238145	35.58132	3.679909	7.451119	0.1549	0.035734	1.234828	0.279417
Max	3.48286467	35.68669	4.109004	9.722516	0.363139	0.043168	1.325762	0.287759
Mean	3.11170154	35.6241	3.866048	8.710105	0.196548	0.037212	1.272979	0.283123

Table 11 Overall Hazard quotients (HQ_{inh}) results of adult population for inhalation pathway

Sample ID	HQ (Pb)	HQ (As)	HQ (Cr)	HQ (Sr)	HQ (Ba)	HQ (zn)	HQ (V)	HQ (Cu)
TSJ 1	1.7489E-10	1.74E-09	2.59E-10	2.26E-09	1.99E-11	1.93E-12	1.59E-10	2.63E-11
TSJ 2	1.5533E-10	1.7E-09	4.59E-10	7.6E-10	1.62E-10	2.5E-12	1.31E-10	2.42E-11
TSJ 3	1.7784E-10	1.72E-09	2.63E-10	2.1E-09	1.09E-11	3.31E-12	1.13E-10	2.39E-11
TSJ 4	1.7156E-10	1.77E-09	3.05E-10	1.96E-09	1.97E-11	2.11E-12	1.28E-10	2.81E-11
TSJ 5	1.4725E-10	1.73E-09	4.32E-10	1.18E-09	2.01E-11	1.94E-12	9.66E-11	2.48E-11
TSJ 6	1.6123E-10	1.7E-09	4.74E-10	1.21E-09	2.62E-11	7.27E-12	1.13E-10	2.74E-11
TSJ 7	1.5312E-10	1.74E-09	3.96E-10	1.58E-09	2.38E-11	1.81E-12	1.13E-10	2.36E-11
TSJ 8	6.2022E-10	7.16E-09	7.13E-10	1.06E-09	1.74E-11	3.62E-12	1.17E-10	1.04E-11
TSJ 9	1.5349E-10	1.71E-09	4.47E-10	1.39E-09	6.44E-11	2.1E-12	9.24E-11	2.32E-11
TSJ 10	4.6378E-10	1.75E-09	5.75E-10	2.08E-09	4.04E-11	4.09E-12	1.3E-10	2.32E-11
Min	1.4725E-10	1.7E-09	2.59E-10	7.6E-10	1.09E-11	1.81E-12	9.24E-11	1.04E-11
Max	6.2022E-10	7.16E-09	7.13E-10	2.26E-09	1.62E-10	7.27E-12	1.59E-10	2.81E-11
Mean	2.3787E-10	2.27E-09	4.32E-10	1.56E-09	4.05E-11	3.07E-12	1.19E-10	2.35E-11

Table 12 Overall Hazard quotients (HQ_{ing}) results of children population for ingestion pathway

Sample ID	HQ (Pb)	HQ (As)	HQ (Cr)	HQ (Sr)	HQ (Ba)	HQ (zn)	HQ (V)	HQ (Cu)
TSJ 1	10.65449011	106.8113	15.677829	133.7392	1.191563	0.117707	9.521394	1.58105
TSJ 2	9.502065666	104.5155	27.473364	45.61136	9.57382	0.151192	7.830205	1.457382
TSJ 3	10.82844097	105.2765	15.880264	124.6068	0.658839	0.199391	6.807035	1.438356
TSJ 4	10.45879539	108.5743	18.366819	116.4891	1.180691	0.128361	7.669626	1.685693
TSJ 5	9.025657752	105.7839	25.880264	70.31963	1.202435	0.118214	5.826146	1.493531
TSJ 6	1.158784842	1.026379	0.7096844	1.656566	0.981917	1.085837	1.316415	1.128662
TSJ 7	7.788898703	103.0651	36.467287	42.44905	1.22458	0.108869	4.425766	1.323275
TSJ 8	0.148773901	0.009959	0.0194608	0.039025	0.80184	9.973783	0.297443	0.852931
TSJ 9	9.39334638	104.7742	26.745053	82.49619	3.811698	0.1276	5.580923	1.400304
TSJ 10	27.67993042	107.3059	34.271943	123.5921	2.398347	0.245053	7.813293	1.400304
Min	0.148773901	0.009959	0.0194608	0.039025	0.658839	0.108869	0.297443	0.852931
Max	27.67993042	108.5743	36.467287	133.7392	9.57382	9.973783	9.521394	1.685693
Mean	9.663918413	84.71431	20.149197	74.0999	2.302573	1.225601	5.708825	1.376149

Table 13 Overall Hazard quotients (HQ_{derm}) results of children population for dermal contact pathway

Sample ID	HQ (Pb)	HQ (As)	HQ (Cr)	HQ (Sr)	HQ (Ba)	HQ (zn)	HQ (V)	HQ (Cu)
TSJ 1	14.57588682	166.4332	17.677116	56.53704	0.865106	0.168687	6.781086	1.409621
TSJ 2	14.33745417	165.9582	20.117572	38.30369	2.599366	0.175615	6.431185	1.384034
TSJ 3	14.61187665	166.1156	17.719	54.64757	0.754887	0.185588	6.219495	1.380098
TSJ 4	14.53539825	166.7979	18.233459	52.96805	0.862856	0.170892	6.397962	1.431271
TSJ 5	14.23888702	166.2206	19.787965	43.41575	0.867355	0.168792	6.016552	1.391514
TSJ 6	14.40943384	165.8532	20.291298	43.83563	0.941584	0.233874	6.21785	1.423398
TSJ 7	14.3104618	166.4305	19.347037	48.34935	0.912342	0.167218	6.221244	1.376162
TSJ 8	14.27447197	166.0107	18.794946	36.17279	0.732393	0.168268	6.399694	1.35648
TSJ 9	14.19799357	165.6433	16.564326	33.12865	0.7099	0.165643	5.521442	1.242324
TSJ 10	18.09839171	166.5355	21.524175	54.43763	1.114785	0.195035	6.427686	1.372225
Min	14.19799357	165.6433	16.564326	33.12865	0.7099	0.165643	5.521442	1.242324
Max	18.09839171	166.7979	21.524175	56.53704	2.599366	0.233874	6.781086	1.431271
Mean	14.75902558	166.1999	19.005689	46.17961	1.036058	0.179961	6.26342	1.376713

Table 14 Overall Hazard quotients (HQ_{inh}) results of children population for inhalation pathway

Sample ID	HQ (Pb)	HQ (As)	HQ (Cr)	HQ (Sr)	HQ (Ba)	HQ (zn)	HQ (V)	HQ (Cu)
TSJ 1	1.48061E-09	1.46E-08	2.221E-09	2E-08	1.74E-10	1.63E-11	1.39E-09	2.28E-10
TSJ 2	1.30529E-09	1.43E-08	4.016E-09	6.61E-09	1.45E-09	2.14E-11	1.14E-09	2.09E-10
TSJ 3	1.50707E-09	1.44E-08	2.252E-09	1.86E-08	9.32E-11	2.87E-11	9.81E-10	2.07E-10
TSJ 4	1.45084E-09	1.49E-08	2.631E-09	1.74E-08	1.73E-10	1.79E-11	1.11E-09	2.44E-10
TSJ 5	1.23282E-09	1.45E-08	3.774E-09	1.04E-08	1.76E-10	1.63E-11	8.32E-10	2.15E-10
TSJ 6	1.35822E-09	1.42E-08	4.144E-09	1.07E-08	2.3E-10	6.42E-11	9.8E-10	2.38E-10
TSJ 7	1.28545E-09	1.46E-08	3.449E-09	1.4E-08	2.09E-10	1.52E-11	9.82E-10	2.04E-10
TSJ 8	1.28875E-09	1.43E-08	3.905E-09	1.22E-08	5.73E-10	1.78E-11	7.94E-10	2.01E-10
TSJ 9	4.07069E-09	1.47E-08	5.05E-09	1.85E-08	3.58E-10	3.56E-11	1.13E-09	2.01E-10
TSJ 10	2.07E-09	1.44E-08	4.05E-09	1.87E-08	4.58E-10	4.56E-11	1.23E-09	2.71E-10
Min	1.23282E-09	1.42E-08	2.221E-09	6.61E-09	9.32E-11	1.52E-11	7.94E-10	2.01E-10
Max	4.07069E-09	1.49E-08	5.05E-09	2E-08	1.45E-09	6.42E-11	1.39E-09	2.71E-10
Mean	1.70504E-09	1.45E-08	3.549E-09	1.47E-08	3.89E-10	2.79E-11	1.06E-09	2.22E-10

Carcinogenic health risk evaluation

The cancer risk (CR) and lifetime cancer risks (LCR) of four carcinogenic trace elements (Pb, As, Sr, Cr) were computed (Table 15). These carcinogenic elements were considered based on their high carcinogenic health risk index in the toxicological profile, as per the International Agency for Research on Cancer (IARC, 2011) and Integrated Risk Information System (IRIS, 2011). In this study, the LCR and CR for both children and adult populations were computed for the three exposure pathways. CR and LCR values of less than 1.0E−06 indicate negligible cancer risk, while values above 1.0E− 04 are indicative of adverse human exposure to cancer risks (US-EPA 2017). Accordingly, an observation of Table 8 shows that cancer risks from ingestion (Cr_{ing}**)** and dermal contact (Cr_{derm}) for both children and adults are relatively higher than the required range (> 1.0E −04). However, cancer risk due to inhalation of dust (Cr_{inh}) occurred within a negligible range (< 1.0E− 04). Based on their mean values the cancer risks (CR) for all the carcinogens for all the exposure routes decreased in the order of As > Cr > Pb > Sr, for both children and adult population sizes. Higher CR seemed to be recorded for the children population compared to the adult; implying higher susceptibility of children to cancer risks than adults. This has been attributed to a greater body weight of adults compared to children in terms of risk exposure (US-EPA 2017; Omeka et al. 20022a). The LCR showed a similar trend of occurrence of carcinogens compared to the CR: Arsenic (As) showed higher LCR values amongst all considered carcinogens for both population sizes, with the children population showing the higher vulnerability of lifetime exposure to all carcinogens (Table 15). The implication of this is that Arsenic and Chromium are the two priority toxic metals (carcinogens) posing the highest health risks to inhabitants of the mining district.

So far, results of human health risk evaluation have shown that risk exposure due to ingestion and dermal contact seems to be the most likely prevalent exposure pathways to toxic elements in the Tashan Jatau mine district. Since agriculture (subsistence farming and animal husbandry) and mining serves the major occupation of the area, inhabitants may be exposed to toxic elements ingestion and dermal contact directly through consumption of crops, cultivation of land and mining activities, thereby constituting a soil-plant-animal-human toxic element exposure pathway. The high-risk level of toxic element exposure to the children population compared to the adult as observed in this area has been attributed to the smaller body weights of the children. Results from this study are in commensuration with those observed in other parts of the world (Jia et al., 2018; Jahromi et al., 2020).

Table 15 Descriptive statistical summary results of cancer risk (CR) and lifetime cancer risk (LCR) assessment of selected carcinogens

		ADULTS				CHILDREN			
Carcinogen	**Statistics**	**Cr_{ingest}**	**Cr_{inh}**	**Cr_{derm}**	**LCR (Adult)**	**Cr_{ingest}**	**Cr_{inh}**	**Cr_{derm}**	**LCR (Children)**
Pb	Min	0.001719	1.2516E-12	0.025945242	2.02E-11	0.076718091	1.04789E-11	0.120683	1.38E-10
	Max	0.005378	5.2718E-12	0.02960435	0.264495	0.235279409	3.46009E-11	0.153836	1.254517
	Mean	0.002223	2.0219E-12	0.026449463	0.095576	0.098549174	1.38254E-11	0.125452	0.74667
As	Min	3.494907	2.544E-09	53.37197928	3.41E-08	156.0121766	2.12797E-08	248.4649	2.2E-07
	Max	3.652968	1.0744E-08	53.5300404	534.3614	162.8614916	2.40322E-08	250.1969	2492.998
	Mean	3.55202	3.4092E-09	53.43614331	189.9605	158.792618	2.19605E-08	249.2998	1360.308
Cr	Min	0.177386	1.2957E-10	1.839954631	2.16E-09	7.838914257	1.11072E-09	8.282163	1.81E-08
	Max	0.391933	3.5663E-10	2.054502108	19.33024	17.13597159	2.52508E-09	10.76209	118.7192
	Mean	0.270455	2.1612E-10	1.933023943	7.344929	11.87191781	1.8146E-09	9.502845	71.24921
Sr	Min	0.001201	1.1403E-12	0.011176679	751.0927	0.052968037	9.91738E-12	0.049693	2.22E-10
	Max	0.004608	3.3833E-12	0.014583774	1502.09	0.200608828	3.00277E-11	0.084806	1.348021
	Mean	0.00309	2.338E-12	0.013065158	0.05385	0.134802131	2.2231E-11	0.069269	0.680239

CONCLUSIONS AND RECOMMENDATION

In the current study, the geochemistry of the Tashan Jatau gold mine province in Northwestern Nigeria, potential sources and degrees of pollution, and interactions between trace elements and oxides were investigated. The potential health risk implications from toxic metal exposure on different population sizes have also been addressed using several environment route/receptor pathways. Based on the numerous research findings, the following conclusions have been drawn:

- Results of a geochemical analysis from XRF and ICP-MS revealed that the soils are characterized by elevated concentrations of V, Cr, Cu, Sr, Zr, Zn and Pb when compared to the upper continental crust and average crustal values. The anomalous concentration and high variability of trace element distribution in the soil are attributed to both anthropogenic inputs (such as mining) and geogenic and surface environmental conditions (such as mobility potential, leaching metal-complexation, weathering and oxidation of parent material)

- Results from parametric multivariate statistical assessment revealed that the distribution and association of trace elements and oxides in the surface soil showed similarity in geochemical behaviour, indicating that they occurred from a common source possibly from the same parent material and elevated by mining activities.

- The quantitative soil pollution indices of contamination factor and enrichment factor revealed that the soils around the mine province are highly contaminated from numerous geogenic processes and anthropogenic inputs, with Cr, V, Cu, Zr, Sr and Ta attributed to anthropogenic inputs while Ba, Zn, Pb, As, Y, Nb, Hf, Sn, Sb, and Sc enrichment was from the parent material.

- The daily dose exposure to risks, hazard quotient and hazard index revealed that the inhabitants are generally more exposed to higher risks from toxic elements ingestion than inhalation and dermal contact; with the children population showing more vulnerability to risk levels than adults.

- The cancer risks (CR) and lifetime cancer risk (LCR) evaluation revealed that cancer risks from ingestion and dermal contact for both children and adults are relatively higher (> 1.0E −04), than the required range. However, cancer risk due to inhalation of dust (Cr_{inh}) occurred within a negligible range (< 1.0E− 04). Higher CR and LCR were recorded for the children population compared to the adult; implying higher susceptibility of children to cancer risks than adults. This has been attributed to the smaller body weight of children compared to adults with respect to risk exposure Arsenic and Chromium were, therefore, identified as the two priority toxic metals (carcinogens) posing the highest health risks to inhabitants of the mining district.
- Agricultural activities (land tilling), artisanal mining, and consumption of unwashed/improperly processed food crops from adjacent farmlands, were the possible direct sources of toxic element exposure to the inhabitants.

It is therefore recommended that source control measures and proper treatment of mine waste effluents be implemented to reduce the risk of human exposure. Proper mining and waste management practices should be implemented and properly regulated. Moreover, an in-depth trace element geochemical evaluation and risk assessment of other valued environmental components such as water, air and plants should be carried out. To further evaluate the long-term effects of toxic elements on the human health system, an analysis of the human tissues is highly recommended.

REFERENCES

Adamu, C. I., Omang, B. O., Oyetade, O. P., Johnson, O. and Nganje, T. N., 2021. Trace and rare earth element geochemistry of the black and grey shales of the Calabar flank, Southeastern Nigeria: constraints on the depositional environment and the degree of metal enrichment. Acta Geochimica, 40(3), 312-324. https://doi.org/10.1007/s11631-020-00434-2

Adepoju-Bello, A. A., Ojomolade, O. O., Ayoola, G. A., and Coker, H. A., 2009. Quantitative analysis of some toxic metals in domestic water obtained from Lagos metropolis, The Nigerian Journal. Pharmacology, 42(1), 57–60

Agency for toxic substances and Disease Registry ASTDR, 2018 Toxicological Profle for hazardous substances. US Department of Health and Human Service

Akoto, O., Ephramin, J. H., and Darko, G., 2008. Heavy metals pollution in surface soils in the vicinity of abundant railway serving workshop in Kumassi, Ghana, International Journal of Environmental Research, 2, 359–364

Benhaddya, M. L., and Hadjel, M., 2014. Spatial distribution and contamination assessment of heavy metals in surface soils of Hassi Messaoud, Algeria, Environmental Earth Sciences, 71, 1473–1486. https://doi.org/10.1007/s12665-013-2552-3

Bhutiani, R., Kulkarni, D. B., Khanna, D. R., and Gautam, A., 2017. Geochemical distribution and environmental risk assessment of heavy metals in groundwater of an industrial area and its surroundings, Haridwar, India, Energy, Ecology and Environment, 2(2), 155–167

CCME (Canadian Council of Ministers of the Environment), 1999. Canadian environmental quality guidelines. Soil Quality Guidelines for the Protection of Environmental and Human Health. Last updated 2007

DPR Department of Petroleum Resources. (Ministry of Petroleum and Natural Resources, Abuja, 2002).

EA (British Environment Agency), 2009. Land contamination: Soil guideline values (SGVs). Science Report SC050021, Bristol, UK. https://www.gov.uk/government/publications/ land-contamination-soil-guideline-valuessgvs publications/ land-contamination- soil-guideline-valuessgvs. Accessed 24 Nov 2014.

Egbueri, J. C., Ukah, B. U., Ubido, O. E., Unigwe, C. O., 2020. A chemometric approach to source apportionment, ecological and health risk assessment of heavy metals in industrial soils from southwestern Nigeria, International Journal of Environmental Analytical Chemistry, 1–19. https://doi.org/10.1080/03067319.2020.1769615.

El-Amari, K., Valera, P., Hibti, M., Pretti, S., Marcello, A., and Essarraj, S., 2014. Impact of mine tailings on surrounding soils and ground water: Case of Kettaraold mine, Morocco, Journal of African Earth Sciences, 100, 437–449. https://doi.org/10.1016/j.jafrearsci.2014.07.017

Funtua I. I., 2001. Elemental compo of Sn-Nb Tg. Mine Tailings from Jos Area, Central Nigeria, Chemie Erde, 56, 45-53

Goldschmidt, V.M., 1937. The principles of distribution of chemical elements in minerals and rocks. The seventh Hugo Müller Lecture, delivered before the Chemical Society on March 17th, 1937, Journal of the Chemical Society (Resumed), 655-673. https://doi.org/10.1039/JR9370000655.

Hakanson, L., 1980. An ecological risk index for aquatic pollution control. A Sedimentological Approach, Water Resources, 14, 975–1001.

Ho, Y.B. and Tai, K.M., 1988. Elevated levels of lead and other metals in roadside soil and grass and their use to monitor aerial metal depositions in Hong Kong, Environmental pollution, 49(1), pp.37-51.. doi:10.1016/0269-7491(88)90012-7.

IARC., 2011. Overall evaluations of carcinogenicity to humans: as evaluated in IARC monographs volumes 1–82 (at total of 900 agents, mixtures and exposures). International Agency for Research on Cancer, Lyon

Jahromi, M. A., Jamshidi-Zanjani, A., and Darban, A. K., 2020. Heavy metal pollution and human health risk assessment for exposure to surface soil of mining area: A comprehensive study, Environmental Earth Sciences, 79(14), 1–18. https://doi.org/10.1007/s12665-020-09110-3.

Jamshidi-Zanjani, A., Saeedi, M., and Li, L. Y., 2015. A risk assessment index for bioavailability of metals in sediments: Anzali International Wetland case study, Environmental Earth Sciences, 73, 2115–2126. https://doi.org/10.1007/s12665-014-3562-5

Jia, Z., Li, S., and Wang, L., 2018. Assessment of soil heavy metals for eco-environment and human health in a rapidly urbanization area of the upper Yangtze Basin, Scientific Reports, 8(1), 1–14. https://doi.org/10.1038/s41598-018-21569-6

Kaiser, H., 1960. The application of electronic computers to factor analysis, Educational and Psychological Measurement, 20, 141–151. https://doi.org/10.1177%2F001316446002000116

Khan, M. U., Malik, R. N., and Mohammed, S., 2013, Human health risk assessment from heavy metal via food crops consumption with wastewater irrigation practices in Pakistan, Chemosphere, 93, 2230–2238. https://doi.org/10.1016/j.chemosphere.2013.07.067

Kim, K. R., Owens, G., and Naidu, R., 2009. Heavy metal distribution, bioaccessibility, and phytoavailability in longterm contaminated soils from Lake Macquarie, Australia, Australian Journal of Soil Resources, 47, 166–176. https://doi.org/10.1071/SR08054.

Krishna, A. K., and Mohan, K. R., 2016. Distribution, correlation, ecological and health risk assessment of heavy metal contamination in surface soils around an industrial area, Hyderabad. India, Environmental Earth Sciences, 75(5), 411. https://doi.org/10.1007/s12665-015-5151-7.

Li, L. Y., Hall, K., Yi, Y., Mattu, G., McCallum, D., and Chen, M., 2009. Mobility and bioavailability of trace metals in the water-sediment system of the highly urbanized brunette watershed, Water, Air, and Soil Pollution, 197, 249– 266. https://doi.org/10.1007/s11270-008-9808-7.

Lü, J., Jiao, W. B., Qiu, H. Y., Chen, B., Huang, X. X., and Kang, B., 2018. Origin and spatial distribution of heavy metals and carcinogenic risk assessment in mining areas at You'xi County southeast China, Geoderma, 310, 99–106. https://doi.org/10.1016/j.geoderma.2017.09.016.

Lu, X., Zhang, X., Li, L.Y. and Chen, H., 2014. Assessment of metals pollution and health risk in dust from nursery schools in Xi'an, China, Environmental research, 128, 27-34.

Migaszewski ZM, Gałuszka A., 2015. The characteristics, occurrence, and geochemical behavior of rare earth elements in the environment: a review, Crit. Rev. Environ. Sci. Technol. 45:429–471. https://doi.org/10.1080/10643389.2013.866622.

Mustapha, A.,2012. Application of principal component analysis and multiple regression models in surface water quality assessment, Journal of Environmental Science, 2(2), 16–23.

Nehls, G. J. and Akland, G. G., 1973. Procedures for handling aerometric data, J. Air Pollut. Control Assoc. 23(3), 180–4 .https://doi.org/10.1080/00022470.1973.10469762.

Nganje, T. N., Adamu, C. I., and Ukpong, E. E., 2010. Heavy metal concentrations in soils and plants in the vicinity of Arufu lead–zinc mine, Middle Benue Trough, Nigeria, Chinese Journal of Geochemistry, 29, 167–174. https:// doi.org/10.1007/s11631-010-0167-x

Nganje, T. N., Adamu, C. I., Ekwere, A. S., Ibe, K. A., Edet, A., and Hursthouse, A. S., 2021. Environmental geochemical signature of shale in pollution assessment of trace metals in soil and water in parts of southern Benue trough, southeastern Nigeria, International Journal of Environmental Analytical Chemistry, 1–21. https://doi.org/10.1080/03067319.2021.1900144.

Obiora, S. C., Chukwu, A., Toteu, S. F., and Davies, T. C., 2016. Assessment of heavy metal contamination in soils around lead (Pb)-zinc (Zn) mining areas in Enyigba, southeastern Nigeria, Journal of Geology Society of India, 87, 453–462.

Okamkpa, J. R. Omeka M. E., Igwe, O. and Iyiokwu M. U., 2022. An integrated geochemical and spatiotemporal assessment of groundwater resources within an industrial suburb, Southeastern Nigeria, International Journal of Energy and Water Resources, 1-20. https://doi.org/10.1007/s42108-022-00183-3

Okon E. E, Kudamnya E. A,Oyeyemi K. D., Omang B. O., Ojo O, Metwaly M: Field Observations and Geophysical Research Applied to the Detection of Manganese (Mn) Deposits in the Eastern Part of Oban Massif, South-Eastern Nigeria: An Integrated Approach. Minerals 2022, 12, 1250. https://doi.org/10.3390/ min12101250

Olade, M. A., 1976. On the genesis of Pb-Zn deposits in Nigeria's Benue Rift (Aulagogen): A reinterpretation, Journal of Mining Geology, 13, 20–27.

Omang, B. O., Asinya, E.A., Udinmwen, E. and Oyetade, O.P., 2022. Structural framework and deformation episodes in the Igarra schist belt, Southwestern Nigeria. Global Journal Series, 20(1), pp.1-17.

Omeka, M. E., and Igwe, O., 2021. Heavy metals concentration in soils and crop plants within the vicinity of abandoned mine sites in Nigeria: an integrated indexical and chemometric approach, International Journal of Environmental Analytical Chemistry, 1-19. https://doi.org/10.1080/03067319.2021.1922683

Omeka, M. E., Egbueri, J. C., and Unigwe, C. O., 2022b. Investigating the hydrogeochemistry, corrosivity and scaling tendencies of groundwater in an agrarian area (Nigeria) using graphical, indexical and statistical modelling, Arabian Journal of Geosciences, 15(13), 1-24. https://doi.org/10.1007/s10661-022-09856-2.

Omeka, M. E., Igwe, O., and Unigwe, C. O., 2022a. An integrated approach to the bioavailability, ecological, and health risk assessment of potentially toxic elements in soils within a barite mining area, SE Nigeria, Environmental Monitoring and Assessment, 194(3), 1-30. https://doi.org/10.1080/03067319.2021.1922683.

Omeka, M. E., and Egbueri, J.C., 2022. Hydrogeochemical assessment and health-related risks due to toxic element ingestion and dermal contact within the Nnewi-Awka urban areas, Nigeria, Environmental Geochemistry and health, 1-29. https://doi.org/10.1080/03067319.2021.1922683

Pam, A. A., Sha'Ato, R., and Ofem, J. O., 2013. Contributions of automobile mechanic sites to heavy metals in soil: a case study of north bank mechanic village Makurdi, Benue State, Central Nigeria, Journal of Chemical, Bio- logical and Physical Sciences, 3, 2337–2347.

Pavilonis, B., Grassman, J., and Johnson, G., 2017. Characterization and risk of exposure to elements from artisanal gold mining operations in the Bolivian Andes, Environmental Res, 154, 1–9. https://doi.org/10.1016/j.envres.2016.12.010 .

Potts P.J, Webb P.C., 1992. X-ray fluorescence spectrometry, Journal of Geochemical Exploration, (44)1–3, 251-296. https://doi.org/10.1016/0375-6742(92)90052-A.

Pourret, O., and Hursthouse, A., 2019. It's time to replace the term "Heavy Metals" with "Potentially Toxic Elements" When reporting environmental research, International Journal of Environmental Resources and Public Health, 16(22). https://doi.org/10.3390/ijerph16224446

Qingjie, G., Jun, D., Yunchuan, X., Qingfei, W., and Liqiang, Y., 2008. Calculating pollution indices by heavy metals in ecological geochemistry assessment and a case study in parks of Beijing, Journal of China University of Geo- sciences, 19, 230–241. https://doi.org/10.1016/S1002-0705(08)60042-4.

Rudnick R L, Gao S., 2014. Composition of the continental crust, treatise on Geochemistry (Second Edition), 4, 1. https://doi.org/ 10.1016/B978-0-08-095975-7.00301-6u

Simex, S. A., and Helz, G. R., 1981. Regional geochemistry of trace elements in Chesapeake Bay, Environmental Geology, 3, 315–323. https://doi.org/10.1007/BF02473521

Souri, M. K., Alipanahi, N., Hatamian, M., Ahmadi, M., and Tesfamariam, T., 2018. Elemental Profle of Heavy Metals in Garden cress, Coriander, Lettuce and Spinach, Commonly Cultivated in Kahrizak. South of Tehran-Iran, Open Agriculture, 3, 3237. https://10.0.5.235/opag-2018-0004

Sparks, D. L., 2005. Toxic metals in the environment: The role of surfaces, Elements, 1, 193–197. https://doi.org/10.2113/gselements.1.4.193.

Taylor, S. R., and McLennan, S. M., 1985. The continental crust: its composition and evolution.

Tchounwou, P. B., Yedjou, C. G., Patlolla, A. K., and Sutton, D. J., 2012. Heavy metal toxicity and the environment, Molecular, clinical and environmental toxicology, 133–164

Tyler G., 2004. Rare earth elements in soil and plant systems—a review, Plant Soil, 267:191–206. https://doi.org/10.1007/s11104-005-4888-2

US EPA (United States Environment Protection Agency), 2005. Ecological soil screening level (Eco-SSL) guidance and documents. Washington DC. Available at: http://www.epa.gov/oswer/riskassessment/ecorisk/ecossl. htm. Accessed 24 Nov 2014.

US EPA IRIS (US Environmental Protection Agency)'s Intergrated Risk Information System, 2011. Environmental Protection Agency Region I, Washington DC 20460.US EPA, 2012. http://www.epa.gov/iris

US-EPA (US Environmental Protection Agency). (2017). National recommended water quality criteria-aquatic life criteria table and human health criteria table. https://www. epa.gov.wqc/national-recommended-water-qualitycriteriaaquatic-life-criteria-table. Accessed 25 Oct 2020

Xiaodong, H., Jianhua, W., and Song, H., 2019. Hydrochemical characteristics and quality evaluation of groundwater in terms of health risks in Luohe aquifer in Wuqi County of the Chinese Loess Plateau, northwest China, Human and Ecological Risk Assessment: An International Journal l, 25(1–2), 32–51. https://doi.org/10.1080/10807039.2018.1531693

Zhang, L., Ye, X., Feng, H., Jing, Y., Quyang, T., Yu, X., Liang, R., Gao, C., and Chen, W., 2007. Heavy metal contamination in western Xiamen Bay sediments and its vicinity, China, Marine Pollution Bulletin, 54, 974–982. https://doi.org/10.1016/j.marpolbul.2007.02.010.